HHS Public Access

Author manuscript

J Mol Cell Cardiol Plus. Author manuscript; available in PMC 2024 January 05.

Published in final edited form as:

J Mol Cell Cardiol Plus. 2023 December ; 6: . doi:10.1016/j.jmccpl.2023.100052.

Effects of canagliflozin on myocardial microvascular density, oxidative stress, and proteomic profile☆

Sharif A. Sabe,

Cynthia M. Xu,

Mohamed Sabra,

Dwight D. Harris,

Mark Broadwin,

Krishna G. Bellam,

Debolina Banerjee,

Anny Usheva,

M. Ruhul Abid,

Frank W. Sellke*

Division of Cardiothoracic Surgery, Department of Surgery, Cardiovascular Research Center, Rhode Island Hospital, Alpert Medical School of Brown University, RI, United States of America

Abstract

Introduction: Sodium-glucose cotransporter-2 inhibitors (SGLT2i) are cardioprotective, and canagliflozin (CANA), an SGLT2i, has been shown to improve perfusion, AMPK signaling, and oxidative stress in chronically ischemic myocardium. The aim of this study is to determine the effects of CANA in nonischemic myocardium on coronary collateralization, oxidative stress, and other molecular pathways determined by proteomic profiling.

Methods: Yorkshire swine underwent placement of an ameroid constrictor to the left circumflex artery. Two weeks later, pigs received no drug (CON, n = 8) or 300 mg CANA daily (n = 8). Treatment continued for five weeks, followed by tissue harvest of nonischemic myocardium.

Results: CANA was associated with decreased capillary density (p = 0.05) compared to CON, without changes in arteriolar density. Reduced capillary density did not correlate with reduced perfusion. Oxidative stress was reduced with CANA (22 % decrease). In the CANA group, there was a trend towards increased p-eNOS and eNOS, without a change in p-eNOS/eNOS ratio, p-Akt, Akt, and p-Akt/Akt ratio. There was no change in p-ERK1/2, but a decrease in

* Corresponding author at: Division of Cardiothoracic Surgery, Department of Surgery, Cardiovascular Research Center, Rhode Island Hospital, Alpert Medical School of Brown University, 2 Dudley Street, MOC 360, Providence, RI 02905, United States of America. fsellke@lifespan.org (F.W. Sellke).

☆Presentation: Abstract presented as poster presentation at 2023 American Heart Association Vascular Discovery Scientific Sessions, May 15–18, 2023, Boston, MA.

Declaration of competing interest

The authors declare that they have no known competing financial interests or personal relationships that could have appeared to influence the work reported in this paper.

Supplementary data to this article can be found online at https://doi.org/10.1016/j.jmccpl.2023.100052.

total ERK1/2 and increase in p-ERK1/2/ERK1/2 ratio. There were no changes in expression of p-AMPK, AMPK, with a trend towards increased ratio of p-AMPK/AMPK. Proteomics analysis identified 2819 common proteins, of which 120 were upregulated and 425 were downregulated with CANA. Pathway analysis demonstrated wide regulation of metabolic proteins.

Conclusions: The effects of CANA on myocardial perfusion and AMPK signaling in chronically ischemic myocardium are not found in nonischemic territory, despite attenuation of oxidative stress. Metabolic proteins are widely regulated in nonischemic myocardium with CANA.

Keywords

Angiogenesis; Coronary microvasculature; Proteomics; SGLT2i

1. Introduction

Sodium-glucose cotransporter 2 inhibitors (SGLT2i) have emerged as promising therapeutic agents for patients with cardiac disease. Originally used as antidiabetic agents, SGLT2i were found in clinical trials to improve cardiovascular outcomes in patients with known cardiovascular disease, independent of glycemic control and even the absence of diabetes [1–4]. Due to these benefits, recent guidelines now recommend SGLT2i in patients with heart failure with reduced or preserved ejection fraction regardless of the presence of type 2 diabetes [5]. However, the mechanisms of SGLT2i-derived benefit in cardiovascular disease are still an active area of investigation, and the precise role of these agents in acute and chronic coronary disease is unclear.

There is scarce clinical data on the specific functional and molecular effects of SGLT2i in the setting of myocardial ischemia. Small animal models of acute myocardial ischemia have shown that treatment with SGLT2i canagliflozin improves left ventricular function, reduces infarct size, reduces oxidative stress, and activates AMPK [6–8]. In our large animal model of chronic myocardial ischemia, we previously found that canagliflozin therapy improved cardiac function and mitigated injury to ischemic myocardial territory by improving perfusion, activating AMPK, attenuating fibrosis, and reducing oxidative stress [9]. However, studies are scarce on the effect of SGLT2i on myocardial territory remote to an ischemic insult. Understanding the effects of these agents in nonischemic myocardium is particularly valuable given that changes in remote myocardium are known to play important roles in the cardiac remodeling response to ischemic injury [10,11].

In order to better understand the mechanisms by which canagliflozin provides benefit in the setting of chronic coronary disease, we utilized our large animal model of chronic myocardial ischemia and examined myocardial tissue remote to the ischemic insult. The aim of this study was to determine the effects of canagliflozin in nonischemic myocardium on coronary collateralization, angiogenic signaling, oxidative stress, and other molecular pathways as determined by proteomic profiling.

2. Methods

The data that support the findings of this study are available from the corresponding author upon reasonable request. Mass spectrometry data are available in the iProX public repository (Project ID IPX0006977000).

2.1. Animal model

Sixteen Yorkshire swine (Tufts, Boston, MA) at age 11 weeks old underwent placement of an ameroid constrictor (Research Instruments SW, Escondido, CA) around the left circumflex artery in order to induce chronic myocardial ischemia, via left mini-thoracotomy [9,12,13]. Two weeks after ameroid placement, animals received either daily 300 mg oral canagliflozin (Janssen Pharmaceuticals, Beerse, Belgium) (CANA, n = 8, 4 female, 4 male) or vehicle with no drug (control, n = 8, 3 female, 5 male) based on random assignment. Treatment continued for five weeks, followed by euthanasia and harvest of myocardial tissue from nonischemic territory for analysis. We have previously reported findings in the ischemic myocardial territory in these swine [9]. All experiments were approved by the Institutional Animal Care and Use Committee of the Rhode Island Hospital (#505821), and animals were cared for in coordination with veterinary technicians at Rhode Island Hospital in compliance with the *Principles of Laboratory Animal Care* formulated by the National Society of Medical Research and the *Guide for the Care and Use of Laboratory Animals*.

2.2. Ameroid constrictor placement

All animals underwent placement of an ameroid constrictor to the proximal left circumflex artery as previously described [9]. Pigs received aspirin (10 mg/kg) and cephalexin (30 mg/kg) orally one day preoperatively and five days post-operatively. Pigs received a fentanyl patch (4 μg/kg) just prior to surgery, which was maintained for a total of 72 h. Anesthesia was induced with intramuscular telazol (4.4 mg/kg) and xylazine (2.2 mg/kg). Pigs were intubated for mechanical ventilation, and anesthesia was maintained with inhaled isoflurane (0.75–3.0% minimum alveolar concentration). A left mini-thoracotomy was made, the left circumflex artery (LCx) was identified, the animal was systemically heparinized (80 IU/kg), and the LCx was isolated with a vessel loop The vessel loop was lifted to occlude the LCx for 2 min as confirmed by ST and/or T wave changes on ECG, during which 5 mL of gold microspheres (BioPal, Worcester, MA) were injected into the left atrium. The vessel loop was relaxed to restore flow to the LCx, and ECG changes were allowed to recover to baseline. An ameroid constrictor (Research Instruments SW, Escondido, CA) was sized and placed around the LCx. Nitroglycerin (1 mL) was applied topically over the vessel as needed to reverse vasospasm. The incision was closed in multiple layers. Amiodarone (10 mg/kg) was given as needed for arrhythmias. Intramuscular buprenorphine (0.03 mg/kg) was administered prior to closure.

2.3. Terminal harvest

After five weeks of treatment, pigs underwent a terminal harvest procedure. A femoral pressure catheter was inserted via a 6F sheath to monitor blood pressure. The heart was then exposed through a midline sternotomy. Following cardiac functional measurements, the heart was excised, and myocardial tissue was quickly divided into 16 segments based on

location with respect to the left anterior descending artery and LCx. In all animals, tissue from the same segment, which was the apical segment just adjacent to the left anterior descending artery, was snap frozen in liquid nitrogen for frozen sectioning, immunoblot analysis, and proteomic analysis.

2.4. Immunofluorescence

Immunofluorescence staining was performed as previously described [14]. Briefly, frozen section slides were thawed, fixed with 10 % paraformaldehyde, blocked in 3 % bovine serum albumin (BSA), and incubated with primary antibody to α-smooth muscle actin (α-SMA) at a 1:500 dilution (Abcam, Cambridge, UK) and isolectin B4 conjugated to Alexa Fluor 647 at a 1:100 dilution (Thermo Fisher Scientific, Waltham, MA) overnight at 4 degrees Celsius. After rinsing with PBS, anti-mouse secondary antibody conjugated to Alexa Fluor 594 at a 1:200 dilution (Cell Signaling, Danvers, MA) was applied and allowed to incubate for 1 h at room temperature. Slides were rinsed, and DAPI was applied for 5 min, followed by rinsing and mounting. Images were analyzed at 20× magnification with an Olympus VS200 Slide Scanner (Olympus Corporation, Tokyo, Japan). Image analysis was performed with QuPath software in a blinded fashion [15]. Capillary density was determined by defining positive isolectin B4 staining by thresholding and determining percent of tissue area stained. Arteriolar count was determined by defining positive α-SMA staining by thresholding and determining the number of objects with a minimum size of $100um^2$ per area of tissue section. Catalog numbers are listed in Supplemental Table 1.

2.5. Immunoblotting

Tissue was lysed in radioimmunoprecipitation assay buffer (Boston Bioproducts, Milford, MA), nonischemic myocardial tissue total protein (40 μg) was fractionated on a 4–12 % Bis-Tris gel (ThermoFisher Scientific), transferred to a nitrocellulose or polyvinylidene difluoride membrane (ThermoFisher Scientific, Waltham, MA), and membranes were incubated overnight at 4 degrees Celsius with 1:1000 dilutions of individual rabbit polyclonal primary antibodies to eNOS, phosphorylated (Ser1177) eNOS (p-eNOS), Akt, phosphorylated (Ser473) Akt (p-Akt), extracellular signal-regulated kinase 1/2 (ERK1/2), phosphorylated ERK1/2 (p-ERK1/2), AMPK, phosphorylated (Thr172) AMPK (p-AMPK), catalase, superoxide dismutase 2 (SOD2) (Cell Signaling, Danvers, MA), NADPH oxidase 3 (NOX3), glutathione peroxidase 1 (GPX1) (ProteinTech, Rosemont, IL, USA), and NADPH oxidase 4 (NOX4) (Abcam, Cambridge, MA). Catalog numbers are listed in Supplemental Table 1. All membranes were probed with glyceraldehyde 3-phosphate dehydrogenase (GAPDH) (Cell Signaling, Danvers, MA) to correct for loading error. Membranes were incubated with anti-mouse or anti-rabbit secondary antibodies (Cell Signaling, Danvers, MA) at a 1:2500 dilution, processed for chemiluminescent detection (Thermo Fisher Scientific, Waltham, MA), and captured with a digital camera system (Bio-Rad ChemiDoc MP, Life Science, Hercules, CA). Densitometric analysis of band intensity was performed using National Institutes of Health Image J software.

2.6. Oxyblot analysis

Oxidative stress in nonischemic myocardial tissue was determined using an Oxyblot Protein Oxidation Detection Kit (MilliporeSigma, Burlington, MA). Tissue was lysed in

radioimmunoprecipitation assay buffer (Boston Bioproducts, Milford, MA), and 20 μg of protein sample was denatured with 12 % sodium dodecyl sulfate, subjected to 2,4-dinitrophenylhydrazine solution to derivatize the samples, incubated at room temperature for 15 min, and neutralized with neutralization solution as per the manufacturer's protocol (MilliporeSigma, Burlington, MA). The samples were fractionated on a 4–12 % Bis-Tris gel, transferred to a nitrocellulose membrane, incubated with primary and secondary antibodies provided in the kit, processed for chemiluminescent detection, and captured with a digital camera system (Bio-Rad ChemiDoc MP, Life Science, Hercules, CA). Densitometric analysis of total column band intensity was performed using NIH Image J software.

2.7. Proteomic analysis

Tissue samples were homogenized and proteins were extracted using T-PER tissue lysis buffer (Thermo Fisher Scientific, Waltham, MA). The protein concentration of the homogenates was determined by BCA assay. The samples were buffer exchanged into digestion buffer/TMTpro labeling buffer (100 mM TEAB) via an overnight acetone precipitation. The samples were reduced with DTT, alkylated with IAA, and digested overnight with Trypsin/LysC. A portion of each sample (1 μg) was labeled with TMTpro 16 plex reagent and multiplexed. The multiplexed samples were fractionated into 10 fractions via RP-HPLC (Thermo UltiMate 3000). The fractions were then analyzed via nLC-MS on an EASY-1200 nLC coupled online to an Orbitrap Fusion Lumos where quantification was performed on the MS2 level. The raw data was processed using Thermo Fisher's Proteome Discoverer with an FDR of 0.1 %. A more detailed protocol for proteomics methodology can be reviewed in the Supplementary materials.

2.8. Data analysis

Data from immunoblot, immunofluorescence, and oxyblot analysis are presented as median are reported as median fold change values compared to the average control with interquartile ranges. All two group comparison data were statistically analyzed with Wilcoxon rank-sum test, using R software. Correlation data was analyzed using Spearman's rank correlation coefficient. Probability values <0.05 were considered significant. For proteomic analysis, significant regulation of proteins was defined by a $\log_2$(fold change) of at least 1 and a p-value less than or equal to 0.01. Proteins were normalized to total peptide amount. Pathway analysis performed using ShinyGo 0.76.1 [16].

3. Results

3.1. Canagliflozin therapy does not improve coronary collateralization

There was no difference in coronary arteriolar density between groups ($p = 0.8$). There was reduced capillary density in the canagliflozin-treated group compared to control ($p = 0.05$) (Fig. 1). Among treated swine, decreased capillary density was not correlated with decreased perfusion ($r_s = -0.095$, $p = 0.84$).

3.2. Canagliflozin reduces myocardial protein oxidation

Oxyblot staining demonstrated that total protein oxidation in nonischemic myocardium was decreased in canagliflozin-treated pigs compared to control ($p = 0.028$) (Fig. 2). There were

no significant differences in expression of GPX1 (p = 0.61), NOX3 (p = 0.78), NOX4 (p = 0.78), catalase (p = 0.78), or SOD2 (p = 0.57) in nonischemic myocardium of swine treated with canagliflozin compared to control (Supplemental Fig. 1).

3.3. Canagliflozin has minimal effects on myocardial angiogenic signaling pathways

In nonischemic myocardium of the canagliflozin-treated pigs, immunoblot experiments showed no differences in expression of total AMPK (p = 0.8) or p-AMPK (p = 0.33), though there was a trend towards increased ratio of p-AMPK to AMPK (p = 0.12). CANA was associated with decreased expression of total ERK1/2 (p = 0.002) and increased ratio of p-ERK1/2 to total ERK1/2 (p = 0.001), without changes in p-ERK1/2 expression (p = 0.96). There was a trend towards increased total (p = 0.13) and phosphorylated (p = 0.19) eNOS, without a change in the ratio of p-eNOS to eNOS (p = 0.69) between groups. There were no differences in expression of total (p = 0.38) or phosphorylated (p = 0.96) Akt, or in the ratio of p-Akt to Akt (p = 0.57) between groups (Fig. 3).

3.4. Canagliflozin significantly alters the cardiac proteomic profile and widely regulates proteins related to metabolism

Proteomic analysis identified 2819 common proteins, of which 120 were significantly upregulated and 425 were significantly downregulated with canagliflozin therapy (Fig. 4). Enrichment analysis of significantly upregulated and downregulated proteins revealed modulation of several metabolic pathways (Figs. 4 and 5). Additionally, proteins were regulated involved in cardiac specific processes including cardiac contraction, muscle adaptation, as well as proteins involved in cardiomyopathy (Table 1). A complete list of up- and down-regulated proteins is provided in the data supplement.

4. Discussion

In the present study utilizing our large animal model of chronic myocardial ischemia, we found that in nonischemic myocardial territory, canagliflozin therapy is associated with 1) a decreased capillary density without changes in arteriolar collateralization, 2) minimal changes in angiogenic signaling pathways, 3) decreased total protein oxidative stress, and 4) wide proteomic regulation particularly involving metabolic pathways. These findings may provide important insights into the effects of SGLT2i in normal myocardial tissue.

Our lab has previously demonstrated in this swine model of chronic myocardial ischemia that canagliflozin therapy markedly improved cardiac function [9]. This improvement was likely mediated by several beneficial effects to ischemic myocardial territory including an increase in perfusion to ischemic myocardial territory, activation of AMPK, mitigation of interstitial and perivascular fibrosis, and reduction of oxidative stress [9]. However, it is important to understand the effects of SGLT2 inhibition in myocardial territory remote to ischemic insult, given that changes in remote myocardium are known to play important roles in the remodeling response to ischemic injury [10,11]. Therefore, the current study provides novel insights that may better elucidate the overall changes that occur in myocardial tissue with canagliflozin therapy.

Canagliflozin therapy did not increase microvessel collateralization in nonischemic myocardium, which was unsurprising given the lack of differences in perfusion to that territory [9]. Interestingly, however, there was strong trend towards reduced capillary density in the canagliflozin-treated group compared to control. Canagliflozin has been previously shown to inhibit human endothelial cell proliferation in-vitro, [17] and to impair angiogenesis in ischemic lower limbs in mice [18]. Our group previously reported no changes in capillary density in chronically ischemic myocardium, despite an increase in perfusion to that territory that could be secondary to canagliflozin-mediated vasodilation [9]. The decreased capillary density in myocardium remote to the ischemic insult therefore appeared to not have any deleterious effects on perfusion, perhaps due to compensation by vasodilatory effects or other mechanisms, though further microvessel-specific studies may be warranted to clarify this. Furthermore, total ERK1/2 was decreased in nonischemic myocardium with canagliflozin treatment, though the activated forms of angiogenic molecular signaling markers ERK1/2, Akt, and eNOS were not increased which was also unsurprising given the lack of increased collateralization.

Previous studies have demonstrated that canagliflozin improves AMPK signaling in ischemic myocardial tissue [9,19]. AMPK plays important roles in cardiac contractility, metabolism, mitochondrial function, apoptosis, and autophagy, so activation of this kinase likely contributes to the beneficial cardiovascular benefits seen with canagliflozin therapy [20]. AMPK was markedly improved in chronically ischemic myocardial tissue, though the effect appears to be blunted in nonischemic territory. Despite a trend towards increased activation of AMPK in remote myocardium, it appears that the impact of canagliflozin is more pronounced in ischemic compared to nonischemic territory. It is important to note that the physiological and molecular effects in nonischemic myocardium and ischemic myocardium differ, and therefore the response to canagliflozin is likely to differ. AMPK activation in ischemic myocardium may be helpful in the recovery of ischemic tissue from the ischemic insult, whereas this recovery response may be less necessary in nonischemic tissue.

Oxidative stress is an important mediator of myocardial injury following an ischemic insult, and contributes to adverse remodeling in both ischemic and remote myocardium [21]. We have previously demonstrated that canagliflozin reduces oxidative stress in ischemic tissue [9], and the current study demonstrates that these findings are replicated in nonischemic myocardium as well. We subsequently investigated whether these changes in oxidative stress were due to direct effects in the nonischemic myocardium, or secondary to effects in adjacent ischemic myocardial territory. Specifically, we investigated expression of anti-oxidant markers catalase, SOD2, and GPX1, as well as pro-oxidant markers NOX3 and NOX4, and found no significant differences in expression of these markers in nonischemic myocardium. There may be other mechanisms involved, but these findings suggest that reduction in oxidative stress in nonischemic tissue may be a downstream effect from changes occurring in ischemic myocardium. Nonetheless, overall decrease in oxidative stress throughout the myocardium may contribute to improved cardiac function and remodeling in the setting of chronic myocardial ischemia.

In order to gain a more global understanding of protein regulation within remote myocardial tissue with canagliflozin therapy, we investigated cardiac proteomic regulation in treated vs untreated swine. We found wide regulation of the proteome, particularly affecting proteolytic and metabolic pathways. There was also regulation of proteins involved in cardiac contraction, cardiac muscle adaptation, and cardiomyopathy. Among the most significantly upregulated proteins were proteosomal subunit alpha and beta subtypes, which are integral components of the ubiquitin proteasome system that plays a major role in cell signaling, protein quality control, and protein turnover in normal and dysfunctional myocardial tissue [22]. However, in the setting of oxidative damage with myocardial ischemia, the ubiquitin proteasome system can become dysfunctional thereby leading to poor clearance of defective and reactive signaling proteins [22]. Therefore upregulation of these proteosomal subunits may potentially offset disruption of the ubiquitin proteosomal system in myocardial tissue, though further investigation is warranted to clarify these findings. Canagliflozin was also associated with broad downregulation of proteins related to a number of metabolic pathways, and further investigation into the impact on metabolite generation and energy production would be necessary to better understand the implications of these changes. Our lab's active studies on the effect of canagliflozin on the metabolomic profile in myocardial tissue may provide clarity in this area.

There are several limitations in this study to discuss. Foremost, our study was limited by small sample size in this large animal model, which may have resulted in underpowered analysis, particularly with regard to the trend in decreased capillary density which may have otherwise achieved statistical significance with a larger sample size. Additionally, while proteomics provides an overview of canagliflozin's effects on protein regulation, other -omics data including transcriptomics and metabolomics will provide further clarity on the broad effects of canagliflozin in myocardial tissue. Finally, analysis of myocardial tissue was performed five weeks after treatment, but data is lacking on shorter-term effects of canagliflozin on this model.

5. Conclusions

Although the effects of canagliflozin on myocardial perfusion and AMPK signaling in chronically ischemic myocardium are not seen in nonischemic territory, canagliflozin does improve oxidative stress in remote myocardial tissue. Further, metabolic and proteolytic proteins are widely regulated in nonischemic myocardium with canagliflozin. Therefore, canagliflozin may exert cardiac benefits in the setting of chronic coronary disease by modulating oxidative stress and metabolic signaling in myocardial tissue remote from ischemic injury.

Supplementary Material

Refer to Web version on PubMed Central for supplementary material.

Acknowledgements

We would like to thank the team at the University of Massachusetts Boston Proteomics Core for their contributions to the proteomics analysis, and we would like to thank the veterinary and animal care staff at Rhode Island Hospital for their excellent care of the animals used in this study.

Sources of funding

Funding for this research was provided by the National Heart, Lung, and Blood Institute (NHLBI) 1F32HL160063–01 (S.A.S.); T32 GM065085 (C.M.X.); T32HL160517 (D.D.H., M.B.); 1R01HL133624 (M.R.A.); 2R56HL133624–05 (M.R.A.); R01HL46716 and R01HL128831 (F.W.S.).

References

[1]. Wiviott SD, Raz I, Bonaca MP, Mosenzon O, Kato ET, Cahn A, et al. Dapagliflozin and cardiovascular outcomes in type 2 diabetes. N Engl J Med 2019 Jan 24;380(4):347–57. [PubMed: 30415602]

[2]. Zinman B, Wanner C, Lachin JM, Fitchett D, Bluhmki E, Hantel S, et al. Empagliflozin, cardiovascular outcomes, and mortality in type 2 diabetes. N Engl J Med 2015 Nov 26;373(22):2117–28. [PubMed: 26378978]

[3]. Perkovic V, Jardine MJ, Neal B, Bompoint S, Heerspink HJL, Charytan DM, et al. Canagliflozin and renal outcomes in type 2 diabetes and nephropathy. N Engl J Med 2019 Jun 13;380(24):2295–306. [PubMed: 30990260]

[4]. Inzucchi SE, Kosiborod M, Fitchett D, Wanner C, Hehnke U, Kaspers S, et al. Improvement in cardiovascular outcomes with empagliflozin is independent of glycemic control. Circulation. 2018 Oct 23;138(17):1904–7. [PubMed: 30354665]

[5]. Heidenreich PA, Bozkurt B, Aguilar D, Allen LA, Byun JJ, Colvin MM, et al. 2022 AHA/ACC/HFSA guideline for the management of heart failure: a report of the American College of Cardiology/American Heart Association Joint Committee on Clinical Practice Guidelines. Circulation. 2022 May 3;145(18):e895–1032. [PubMed: 35363499]

[6]. Baker HE, Kiel AM, Luebbe ST, Simon BR, Earl CC, Regmi A, et al. Inhibition of sodium–glucose cotransporter-2 preserves cardiac function during regional myocardial ischemia independent of alterations in myocardial substrate utilization. Basic Res Cardiol 2019 Apr 19;114(3):25. [PubMed: 31004234]

[7]. Sayour AA, Korkmaz-Icöz S, Loganathan S, Ruppert M, Sayour VN, Oláh A, et al. Acute canagliflozin treatment protects against in vivo myocardial ischemia–reperfusion injury in non-diabetic male rats and enhances endothelium-dependent vasorelaxation. J Transl Med 2019 Apr 16;17:127. [PubMed: 30992077]

[8]. Lim VG, Bell RM, Arjun S, Kolatsi-Joannou M, Long DA, Yellon DM. SGLT2 inhibitor, canagliflozin, attenuates myocardial infarction in the diabetic and nondiabetic heart. JACC Basic Transl Sci 2019 Feb;4(1):15–26. [PubMed: 30847415]

[9]. Sabe SA, Xu CM, Sabra M, Harris DD, Malhotra A, Aboulgheit A, et al. Canagliflozin improves myocardial perfusion, fibrosis, and function in a swine model of chronic myocardial ischemia. J Am Heart Assoc 2023 Jan 3;12(1):e028623. [PubMed: 36583437]

[10]. Carrick D, Haig C, Rauhalammi S, Ahmed N, Mordi I, McEntegart M, et al. Pathophysiology of LV remodeling in survivors of STEMI: inflammation, remote myocardium, and prognosis. JACC Cardiovasc Imaging 2015 Jul;8(7):779–89. [PubMed: 26093923]

[11]. Shanmuganathan M, Masi A, Burrage MK, Kotronias RA, Borlotti A, Scarsini R, et al. Acute response in the noninfarcted myocardium predicts long-term major adverse cardiac events after STEMI. JACC Cardiovasc Imaging 2023 Jan;16(1):46–59.

[12]. Scrimgeour LA, Potz BA, Aboul Gheit A, Shi G, Stanley M, Zhang Z, et al. Extracellular vesicles promote arteriogenesis in chronically ischemic myocardium in the setting of metabolic syndrome. J Am Heart Assoc 2019 Aug;6;8(15):012617.

[13]. Aboulgheit A, Karbasiafshar C, Zhang Z, Sabra M, Shi G, Tucker A, et al. Lactobacillus plantarum probiotic induces Nrf2-mediated antioxidant signaling and eNOS expression resulting

in improvement of myocardial diastolic function. Am J Physiol Heart Circ Physiol 2021 Nov 1;321(5):H839–49. [PubMed: 34506225]

[14]. Elmadhun NY, Lassaletta AD, Chu LM, Liu Y, J F, Sellke FW. Atorvastatin increases oxidative stress and modulates angiogenesis in Ossabaw swine with the metabolic syndrome. J Thorac Cardiovasc Surg 2012;144:1486–93. [PubMed: 22995723]

[15]. Bankhead P, Loughrey MB, Fernández JA, Dombrowski Y, McArt DG, Dunne PD, et al. QuPath: open source software for digital pathology image analysis. Sci Rep 2017 Dec 4;7(1):16878. [PubMed: 29203879]

[16]. Ge SX, Jung D, Yao R. ShinyGO: a graphical gene-set enrichment tool for animals and plants. Bioinformatics. 2020 Apr 15;36(8):2628–9. [PubMed: 31882993]

[17]. Behnammanesh G, Durante ZE, Peyton KJ, Martinez-Lemus LA, Brown SM, Bender SB, et al. Canagliflozin inhibits human endothelial cell proliferation and tube formation. Front Pharmacol 2019 Apr 16;10:362. [PubMed: 31057401]

[18]. Lin Y, Nan J, Shen J, Lv X, Chen X, Lu X, et al. Canagliflozin impairs blood reperfusion of ischaemic lower limb partially by inhibiting the retention and paracrine function of bone marrow derived mesenchymal stem cells. EBioMedicine. 2020 Feb;52:102637. [PubMed: 31981975]

[19]. Kondo H, Akoumianakis I, Badi I, Akawi N, Kotanidis CP, Polkinghorne M, et al. Effects of canagliflozin on human myocardial redox signalling: clinical implications. Eur Heart J 2021 Dec 21;42(48):4947–60. [PubMed: 34293101]

[20]. Young LH, Zaha VG. AMP-activated protein kinase regulation and biological actions in the heart. Circ Res 2012 Aug 31;111(6):800–14. [PubMed: 22935535]

[21]. Bugger H, Pfeil K. Mitochondrial ROS in myocardial ischemia reperfusion and remodeling. Biochim Biophys Acta Mol basis Dis 1866;2020 Jul 1(7):165768.

[22]. Calise J, Powell SR. The ubiquitin proteasome system and myocardial ischemia. Am J Physiol Heart Circ Physiol 2013 Feb 1;304(3):H337–49. [PubMed: 23220331]

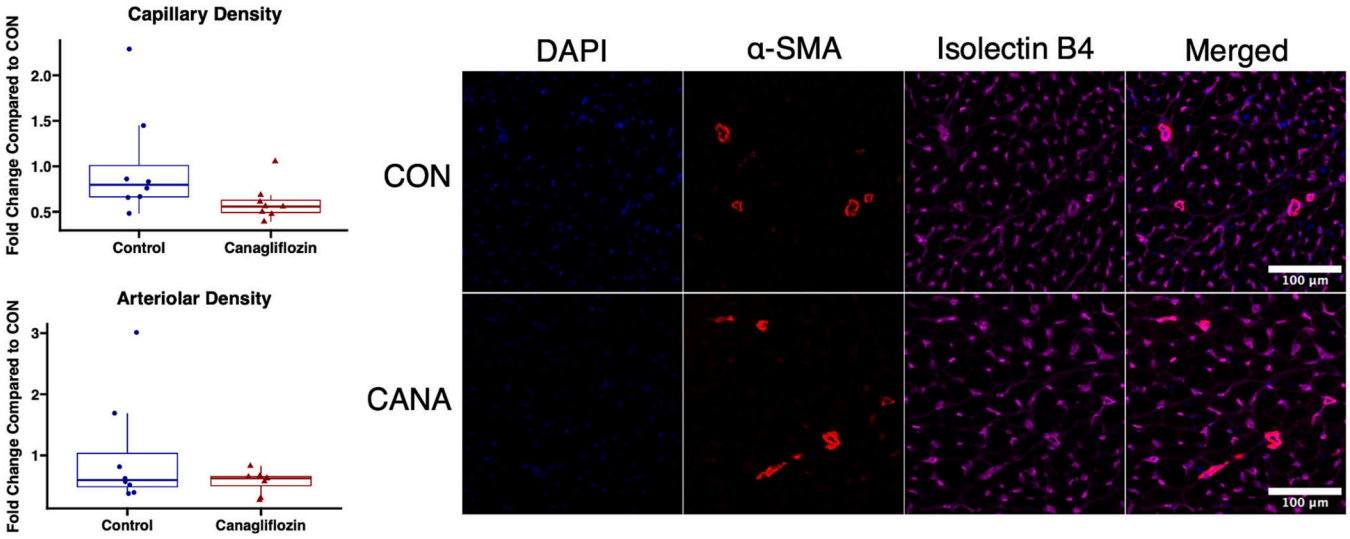

Fig. 1. Canagliflozin therapy does not improve coronary collateralization.

In nonischemic myocardial tissue, there were no significant differences in arteriolar density as determined by α-smooth muscle actin (α-SMA) staining (red), between canagliflozin-treated pigs (CANA, n = 8) and control (CON, n = 8). There was a strong trend towards reduced capillary density as determined by isolectin B4 staining (purple), between CANA and control. Capillary and arteriolar densities were normalized to the average value in the control group. Boxplot upper and lower borders represent upper and lower quartiles, middle horizontal line represents median, upper and lower whiskers represent maximum and minimum values. Representative images of ischemic myocardial tissue are shown on the right.

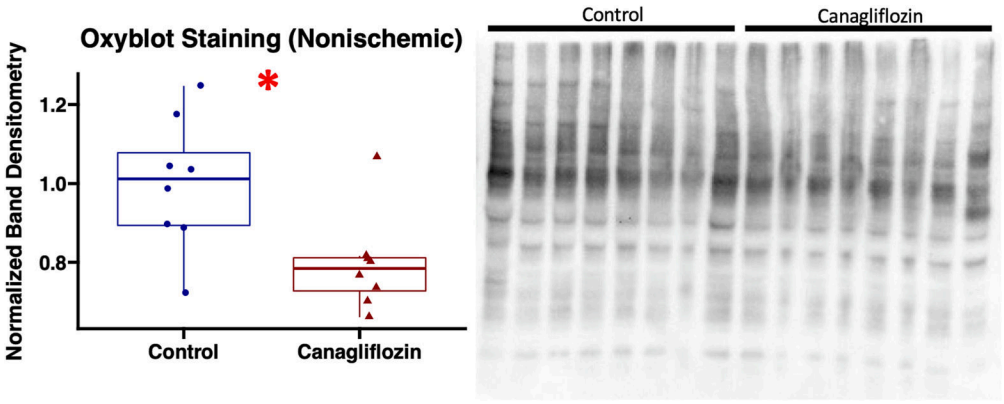

Fig. 2. Canagliflozin reduces myocardial protein oxidation.

Total protein oxidation as measured by Oxyblot staining was decreased in nonischemic myocardial territory in canagliflozin-treated pigs (n = 8) compared to control (n = 8). Band densitometry of entire lane for each sample normalized to average value in control group. Upper and lower borders of box represent upper and lower quartiles, middle horizontal line represents median, upper and lower whiskers represent maximum and minimum values of non-outliers. *$p < 0.05$ as calculated by Wilcoxon rank-sum test.

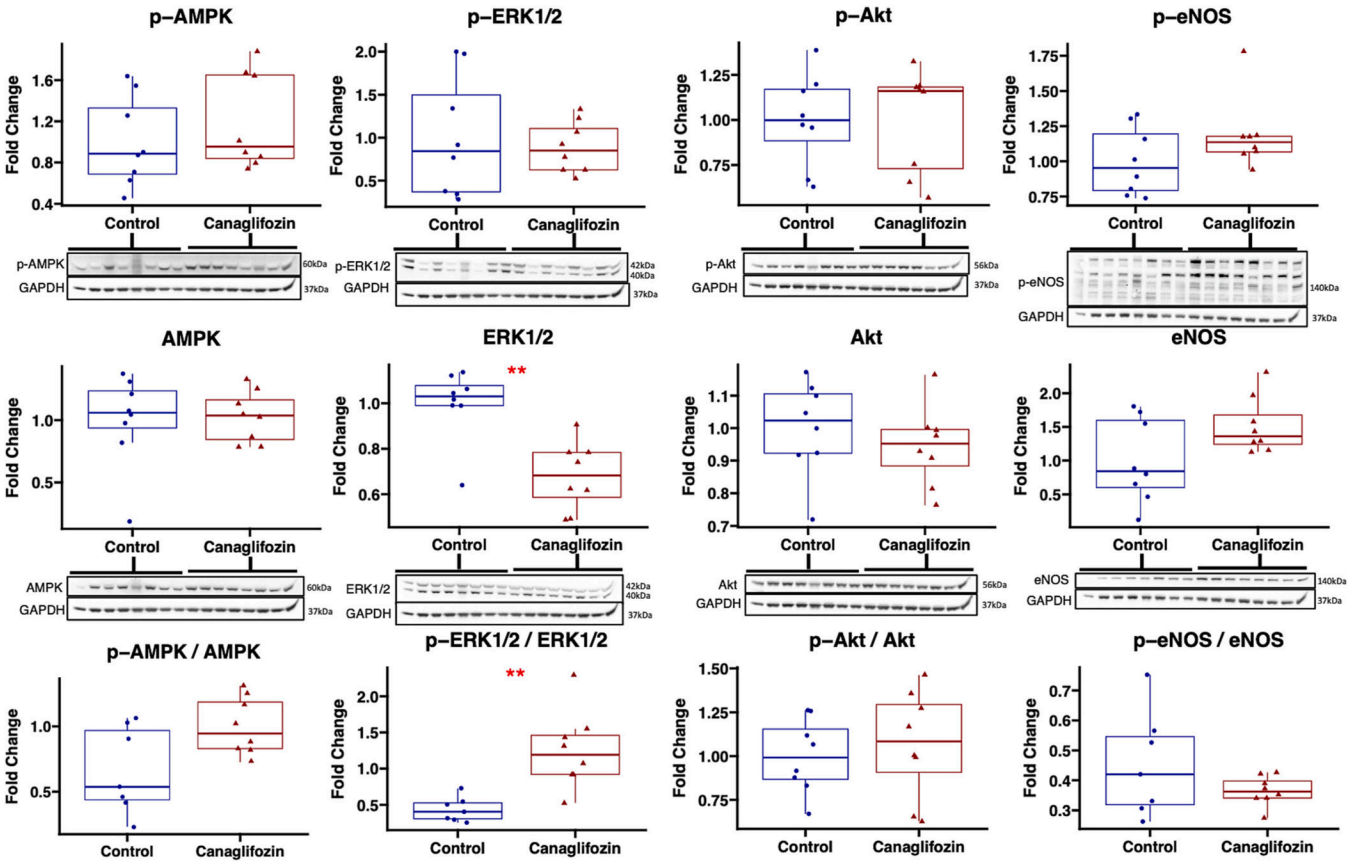

Fig. 3. Canagliflozin has minimal effects on myocardial angiogenic signaling pathways.

Immunoblotting of nonischemic myocardial tissue in canagliflozin-treated pigs (n = 8) and control (n = 8) was performed to quantify differences in protein expression of phosphorylated (p-) and total 5′ adenosine monophosphate-activated protein kinase (AMPK), extracellular signal-regulated kinase 1/2 (ERK1/2), endothelial nitric oxide synthase (eNOS), and Akt expression, as well as their respective ratios. Values expressed as fold change compared to average value in control group. Upper and lower borders of box represent upper and lower quartiles, middle horizontal line represents median, upper and lower whiskers represent maximum and minimum values of non-outliers. *$p < 0.05$, **$p < 0.01$ as calculated by Wilcoxon rank-sum test.

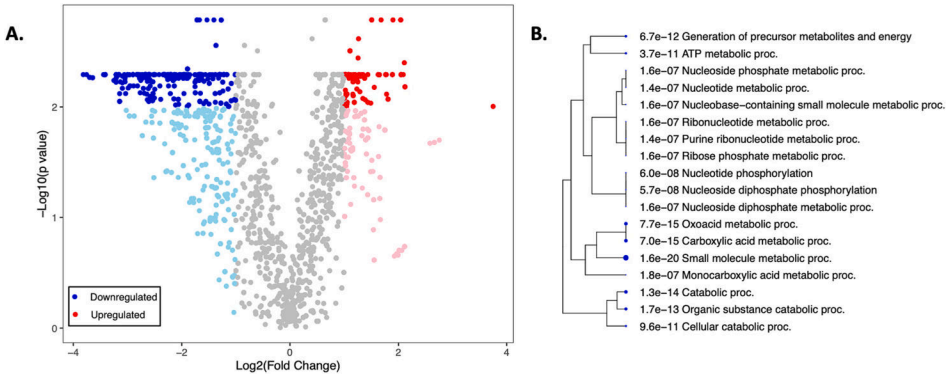

Fig. 4. Canagliflozin significantly alters the cardiac proteomic profile.

Proteomic analysis identified 2819 common proteins, of which 120 were significantly upregulated and 425 were significantly downregulated with canagliflozin therapy (n = 8) compared to control (n = 8). A) Volcano plot (left) generated using $\log_2$(fold-change) threshold of at least 1 and adjusted p-value cutoff of 0.01, with resulting downregulated proteins in blue, and upregulated proteins in red. B) Hierarchical clustering tree (right) highlighting related enriched pathways. Clustering tree created using ShinyGO 0.76.1.

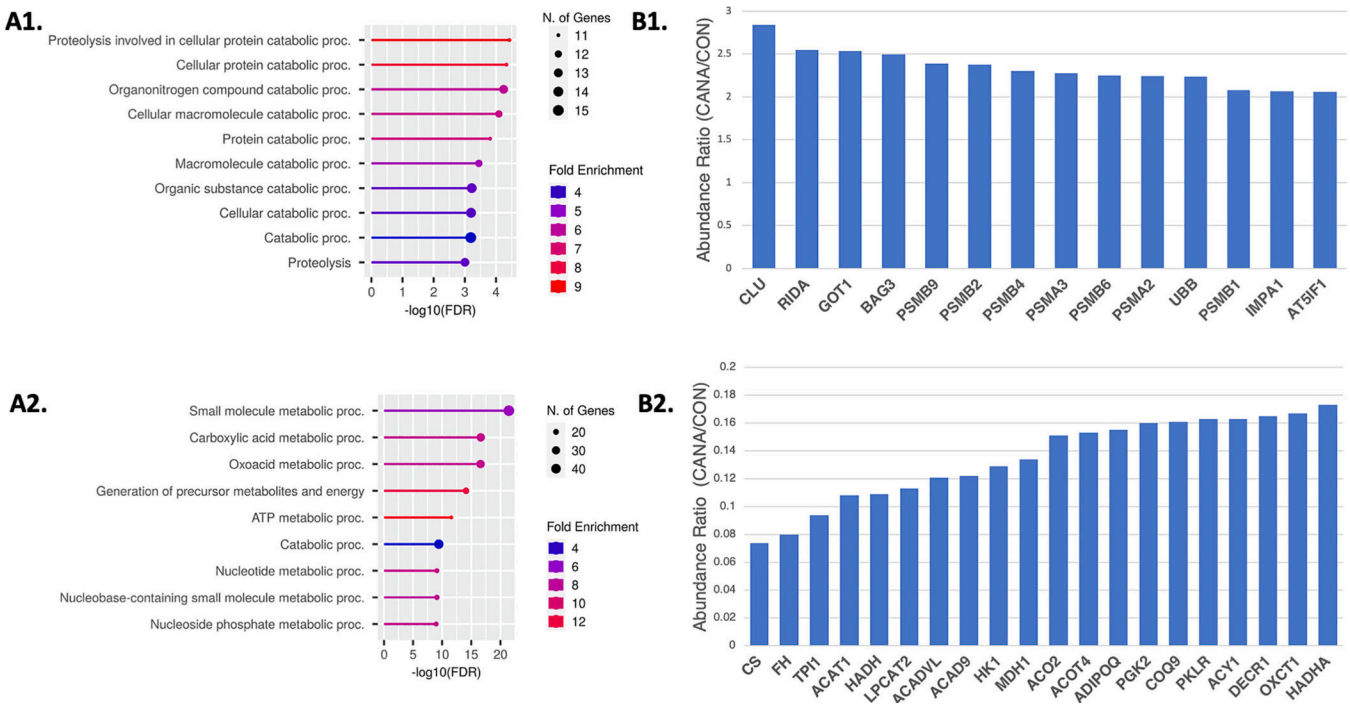

Fig. 5. Proteomic analysis demonstrates that canagliflozin widely regulates proteins related to metabolism.

Proteomic enrichment analysis of significantly A1) upregulated and A2) downregulated proteins revealed modulation in several metabolic pathways. Specific B1) upregulated and B2) downregulated proteins related to metabolic pathways are shown based on their relative abundance ratios. Graphic obtained from ShinyGO 0.76.1. N, number; proc., processes; FDR, false discover rate. CLU, clusterin; RIDA, 2-iminobutanoate/2-iminopropanoate deaminase; GOT1, aspartate aminotransferase, cytoplasmic; BAG3, BAG cochaperone 3; PSMB9, proteasome subunit beta 9; PSMB2, proteasome subunit beta 2; PSMB4, proteasome subunit beta 4; PSMA3, proteasome subunit alpha type 3; PSMB6, proteasome subunit beta 6; PSMA2, proteasome subunit alpha type 2; UBB, ubiquitin B; PSMB1, proteasome 20S subunit beta 1; IMPA1, inositol-1-monophosphatase; AT5IF1, ATP synthase F1 subunit epsilon; CS, citrate synthase, mitochondrial; FH, fumarate hydratase, mitochondrial; TPI1, triosephosphate isomerase; ACAT1, acetyl-CoA acetyltransferase 1; HADH, hydroxyacyl-coenzyme A dehydrogenase, mitochondrial; LPCAT2, lysophosphatidylcholine acyltransferase 2; ACADVL, acyl-CoA dehydrogenase very long chain; ACAD9, acyl-CoA dehydrogenase family member 9; HK1, hexokinase; MDH1, malate dehydrogenase; ACO2, aconitate hydratase; ACOT4, acyl-CoA thioesterase 4; ADIPOQ, adiponectin; PGK2, phosphoglycerate kinase 2; COQ9, ubiquinone biosynthesis protein; PKLR, pyruvate kinase; ACY1, N-acyl-aliphatic-L-amino acid amidohydrolase; DECR1, 2,4-dienoyl-CoA reductase 1; OXCT1, 3-oxoacid CoA-transferase; HADHA, trifunctional enzyme subunit alpha, mitochondrial.

Table 1

Regulated proteins in cardiac processes.

	Gene ID	Protein name
	CACNA2D1	Calcium Voltage-Gated Channel Auxiliary Subunit Alpha2delta
Cardiac contraction	DMD	Dystrophin
	SPTBN4	Spectrin beta chain, non-erythrocytic 4
	CAV3	Caveolin-3
Cardiac muscle adaptation	LMNA	Lamin A/C
	CEP85L	Centrosomal protein 85-like
	LMNA	Lamin A/C
	BAG3	BAG cochaperone 3
	CAT	Catalase
	CD36	Platelet glycoprotein 4
Cardiomyopathy	ACADVL	Very long-chain specific acyl-CoA dehydrogenase, mitochondrial
	DMD	Dystrophin
	CTNNA2	Catenin alpha-2
	CACNA2D1	Calcium voltage-gated channel auxiliary subunit alpha2delta 1
	LAMA2	Laminin subunit alpha-2

Regulated proteins listed based on proteomics analysis organized by cardiac-related processes.